Journal of Thermal Stresses
Publication details, including instructions for authors and subscription information:
http://www.informaworld.com/smpp/title~content=t713723680

Thermal Stress Analysis by Refined Multilayered Composite Shell Theories

S. Brischetto [a]; E. Carrera [a]
[a] Department of Aeronautics and Space Engineering, Politecnico di Torino, Turin, Italy

Online Publication Date: 01 January 2009

To cite this Article Brischetto, S. and Carrera, E.(2009)'Thermal Stress Analysis by Refined Multilayered Composite Shell Theories',Journal of Thermal Stresses,32:1,165 — 186
To link to this Article: DOI: 10.1080/01495730802540882
URL: http://dx.doi.org/10.1080/01495730802540882

Journal of Thermal Stresses, 32: 165–186, 2009

ISSN: 0149-5739 print/1521-074X online
DOI: 10.1080/01495730802540882

Taylor & Francis
Taylor & Francis Group

THERMAL STRESS ANALYSIS BY REFINED MULTILAYERED COMPOSITE SHELL THEORIES

S. Brischetto and E. Carrera
Department of Aeronautics and Space Engineering, Politecnico di Torino, Turin, Italy

This paper considers the thermal stress uncoupled problem of multilayered composite shells. An assumed linear distribution of temperature through the thickness is considered for thicklthin cylindrical and spherical shells including carbon fiber reinforced layers andlor a central soft core. The Carrera's Unified Formulation (CUF) and the Principle of Virtual Displacements (PVD) are extended to derive differential governing equations for the thermal analysis of shells with constant radii of curvature. Classical and refined two-dimensional models are treated in a unified form. Both Equivalent Single Layer (ESL) and Layer-Wise (LW) approaches are considered along with variable order of expansion in the thickness direction, from linear to fourth order. In the case of ESL, the typical zig-zag form of the displacement is accounted for via the Murakami's function. Classical models have also been considered for comparison purposes. The obtained results demonstrate the effectiveness of refined models for a correct evaluation of displacements and stress field in laminated shells.

Keywords: Assigned thermal profile; Carrera's unified formulation; Closed form solutions; Equivalent single layer models; Layer wise models; Multilayered composite shells; Principle of virtual displacements

INTRODUCTION

In the typical aeronautical structures such as multilayered composite plates and shells, the temperature variations are one of the most important factor for the stress fields that cause their failure. Advanced composite materials combine a number of properties, including high specific strength and stiffness, and nearly zero coefficient of thermal expansion in the fiber orientation. These relevant properties result in a growing use of composite materials in structures subjected to severe thermal environment, such as high temperatures, high gradients and cycling changes of temperature. Due to these implications, the effects of both high-temperature and mechanical loadings have to be considered in the design process of such structures

Received 13 May 2008; accepted 8 August 2008.

This paper is devoted to the memory of Professor Liviu Librescu of Virginia Tech who on April 16th 2007 died courageously trying to save his students' lives.

The second author always remembers with immense pleasure the departed time together with Professor Librescu, an extraordinary teacher of science and life.

Address correspondence to Salvatore Brischetto, Department of Aeronautics and Space Engineering, Politecnico di Torino, Corso Duca degli Abruzzi, 24, Torino 10129, Italy, E-mail: salvatore.brischetto@polito.it

[1–3]. An accurate description of local stress fields in the layers becomes mandatory to prevent thermally loaded structures failure mechanisms. For these reasons, increasing work has recently been devoted to the development of computational models for studying the behavior of high-temperature composite plates and shells [3].

Wu and Chen [4] have recently developed a higher-order model to accurately predict the displacements and stresses in laminated shells, in addition the thermal bending is also considered. A Finite Element shell has been developed by Rolfes et al. [5] to analyze the composite structures simultaneously loaded by mechanical and thermal loads, the assigned temperature profile is presumed linear or quadratic in the thickness direction. Assuming a linear-through-the thickness profile of temperature, Khare et al. provided a closed form thermo mechanical solution for laminated and sandwich shells [6]. Different higher-order theories are proposed, among of these, of particular interest is the so called HOST12 (12 parameters, cubic expansion in the z direction for each displacement component). These refined theories are compared with the HSDT (Higher Shear Deformation Theory) by Khdeir et al. [7]. Khdeir has solved exactly the thermoelastic governing equations for laminated shells in [8], the temperature field is again assumed uniform or linearly varying through the thickness. Birsan [9] uses the Cosserat surfaces to analyze the thermal stresses in cylindrical elastic shells by means of two given temperature fields.

The use of Cosserat surfaces is suggested again by Iesan [10], the temperature variation for the composite cylinders is assumed as a polynomial in the axial coordinates. A non-linear thermoelastic analysis with shell elements is proposed by Barut et al. [11] considering a linear temperature profile through the thickness direction. The thermoelastic behavior of composite shells is investigated by means of both closed-form and finite element solution by Hsu et al. [12] using Dong and Tso's laminated shell theory, a weak formulation for the mixed-state equations including the boundary conditions, is given by Ding [13]. A pioneer work about the thermal analysis of layered composite shells is that by Miller et al. [14] that applies a classical shell theory for an arbitrary distribution of temperature through the thickness. An other important aspect of the thermal analysis of laminated shells is the investigation of the effects of the mechanical and thermal anisotropy, as just illustrated by Padovan [15]. The importance of the zig-zag form of displacements in the thermal analysis of composite shells have been remarked by Dumir et al. [16]. An interesting extension of the thermoelastic problems to composite shells, could be the use of piezoelectric layers in order to control the thermal deformations [17]. Some experimental results have been proposed by Holstein et al. [18]. Two different anisotropic composite tubes are experimentally and numerically (by ANSYS) investigated in order to characterize their deformation behavior under thermal load.

Recently, the authors have investigated the thermal effects in composite structures. In [19] a study on the influence of the through-the-thickness temperature profile on the thermomechanical response of multilayered anisotropic thick and thin plates has been addressed. The partially coupled stress problem was considered by solving the Fourier's conductivity equation. The importance of mixed theories for a correct prediction of transverse shear/normal stresses due to thermal loadings have been remarked in [20]. Extension to Functionally Graded Materials (FGMs) has been done in [21].

All the above-mentioned works were restricted to the plate geometry. The present paper extends the thermoelastic formulation to shells. Several hierarchical two-dimensional models, obtained via Carrera's Unified Formulation (CUF) [22], are introduced by means of the Principle of Virtual Displacements (PVD). These classical and refined models consider the temperature as an external load. To point out the importance of refined kinematics in the case of multilayered composite shells [23], the temperature profile is considered always linear through the thickness for each two-dimensional model. A future companion paper would investigate the effects of the calculated temperature profile for thick and thin multilayered composite shells.

UNIFIED FORMULATION

Carrera's Unified Formulation (CUF) [22] permits to obtain a large variety of two-dimensional models in case of bi-dimensional multi-layered structures such as plates and shells. In this section CUF is described for shells of constant thickness h and radii of curvature R_α and R_β. The geometry and reference system are shown in Figure 1. The displacement components u_α, u_β and u_z are measured with respect to α, β and z axes. The latter axis denotes the through-the-thickness direction. Ω is the shell/plate reference surface. In the case of plates, the curvilinear coordinates α and β coincide with the Cartesian ones x and y, being u_x, u_y and u_z the displacement components.

The obtained hierarchical models differ in the order of used expansion in thickness direction and in the manner the variables are modelled (Equivalent Single Layer (ESL) or Layer-Wise (LW) approach). The salient feature of CUF is the unified manner in which all considered variables and fields (displacement, temperature) can be treated. The considered variables and their variation are split in a set of thickness functions and the relative terms depending on in-plane coordinates (α, β) only.

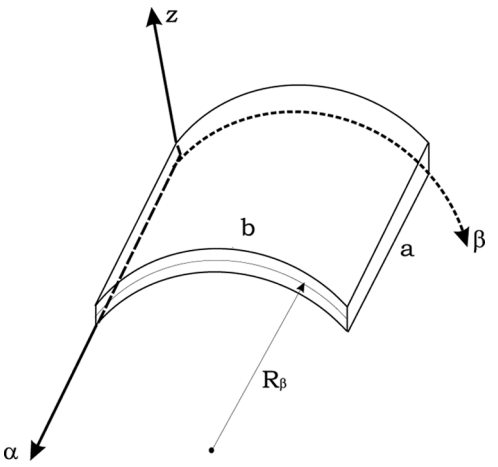

Figure 1 Geometry and notations for a cylindrical shell, particular case of spherical shell when $R_\alpha = \infty$.

According to this separation, a general variable $\boldsymbol{a}$ and its respective variation $\delta\boldsymbol{a}$ can be written as:

$$\boldsymbol{a}(\alpha, \beta, z) = F_\tau(z)\boldsymbol{a}_\tau(\alpha, \beta), \quad \delta\boldsymbol{a}(\alpha, \beta, z) = F_s(z)\delta\boldsymbol{a}_s(\alpha, \beta) \quad \text{with} \quad \tau, s = 1, \ldots, N \quad (1)$$

where N is the order of expansion in the thickness direction.

Equivalent Single Layer Theories

The Equivalent Single Layer (ESL) models are based on the assumption of a global description of the displacement field along the whole shell thickness; a Taylor expansion is used:

$$\boldsymbol{u}(\alpha, \beta, z) = F_\tau(z)\boldsymbol{u}_\tau(\alpha, \beta) = z^r\boldsymbol{u}_r(\alpha, \beta), \quad r = 0, 1, 2, \ldots, N \quad (2)$$

where the displacement vector is $\boldsymbol{u} = (u_\alpha, u_\beta, u_z)$.

The summing convention for the repeated indexes has been adopted. N is the order of expansion, which is taken as a free parameter. In the numerical investigation N is considered to be as low as 1 and as high as 4. According to the acronym system developed within CUF, the related theories are named ED1-ED4. The letter E denotes that the kinematic is preserved for the whole layers, as in the ESL approach. D denotes that only displacement unknowns are used and the last number states the through-the-thickness expansion order ($N = 1, \ldots, 4$).

Classical models such as the First order Shear Deformation Theory (FSDT) and the Classical Lamination Theory (CLT) are obtained from ED1, by imposing a constant through the thickness transverse displacement and considering an infinite shear factor (CLT). For each theory with constant or linear transverse displacement (CLT, FSDT and ED1), the plane-stress conditions are imposed as illustrated in [24, 25] to avoid Poisson's locking phenomena.

Murakami's Zig-Zag Function

The EDN models are not able to describe the discontinuity of the first derivative with correspondence to the layer interfaces, known as zig-zag effects and peculiar of laminate mechanics. It can be introduced via the Murakami's Zig-Zag Function (MZZF) [26], which was proposed in the framework of [27] and [28]. The dimensionalized layer coordinate $\zeta_k = (2z_k)/h_k$ is further introduced, being h_k the thickness of the kth layer and z_k the layer thickness coordinate. MZZF is defined according to the following formula:

$$\text{MZZF} = (-1)^k\zeta_k. \quad (3)$$

MZZF has the following properties: it is piecewise linear function of the layer coordinate z_k; it has unit amplitude for the whole layers; its slope assumes opposite sign between two-adjacent layers, because its amplitude layer is thickness independent. The displacement field accounting for MZZF assumes the following form:

$$\boldsymbol{u}(\alpha, \beta, z) = \boldsymbol{u}_0(\alpha, \beta) + z^r\boldsymbol{u}_r(\alpha, \beta) + (-1)^k\zeta_k\boldsymbol{u}_Z(\alpha, \beta) \quad \text{with} \quad r = 1, 2, \ldots, N-1 \quad (4)$$

Subscript Z refers to the introduced zig-zag term. Higher order distributions in the z-direction are introduced by the r-order polynomials. Modifications of EDN directed to include MZZF are herein denoted as EDZN analysis. In EDZ1 the Poisson's locking phenomena is contrasted according to [24, 25].

Layer-Wise Theories

Multilayered plates and shells can be analysed by kinematic assumptions which are independent in each layer. According to Reddy [29] these approaches are herein stated as Layer-Wise (LW) theories. LW description yields, thus, displacement variables that are independent in each layer. Taylor's thickness expansion, adopted in the previous paragraphs for ESL cases, is not convenient for LW description. Displacements interlaminar continuity can be imposed more conveniently by employing interface values as unknown variables. LW description assumes to the following form:

$$\begin{aligned}\boldsymbol{u}^k(\alpha,\beta,z) = {} & F_t(z)\boldsymbol{u}_t^k(\alpha,\beta) + F_b(z)\mathbf{u}_b^k(\alpha,\beta) \\ & + F_r(z)\boldsymbol{u}_r^k(\alpha,\beta), \quad r = 2,3,\ldots,N, \;\; k = 1,2,\ldots,N_l \end{aligned} \tag{5}$$

N_l indicates the number of layers. Subscripts t and b denote values related to the top and the bottom of each layer, respectively. The thickness functions $F_\tau(\zeta_k)$ have been defined by:

$$F_t = \frac{P_0 + P_1}{2}, \quad F_b = \frac{P_0 - P_1}{2}, \quad F_r = P_r - P_{r-2}, \quad r = 2,3,\ldots,N \tag{6}$$

in which $P_j = P_j(\zeta_k)$ is the Legendre's jth-order polynomial defined in the ζ_k–domain: $-1 \le \zeta_k \le 1$. In the numerical investigations the maximum order is considered to be four, related polynomials are:

$$P_0 = 1, \quad P_1 = \zeta_k, \quad P_2 = (3\zeta_k^2 - 1)/2, \quad P_3 = \frac{5\zeta_k^3}{2} - \frac{3\zeta_k}{2}, \quad P_4 = \frac{35\zeta_k^4}{8} - \frac{15\zeta_k^2}{4} + \frac{3}{8}$$

The previous functions have the following interesting properties:

$$\zeta_k = \begin{cases} 1 : F_t = 1; F_b = 0; F_r = 0 \\ -1 : F_t = 0; F_b = 1; F_r = 0 \end{cases} \tag{7}$$

The top and bottom values have been used as unknown variables. The interlaminar compatibility of displacement can be therefore easily linked:

$$\boldsymbol{u}_t^k = \boldsymbol{u}_b^{(k+1)}, \quad k = 1, \;\; N_l - 1 \tag{8}$$

The acronyms for these theories are LD1-LD4, signifying L Layer-Wise approach.

Temperature Profile

In the proposed thermal bending problems, the assigned temperature profile through the thickness of the shell is always linearly varying. For each proposed kinematic model the temperature profile is approximated LW by using the Legendre's polynomial that have the property to assume the value 1 at the top and bottom of each layer. So imposed the values of temperature at the top and bottom of each layer of the shell, the temperature profile is known.

$$T^k(\alpha, \beta, z) = F_\tau(z)\theta^k_\tau(\alpha, \beta), \quad \tau = 0, 1, \ldots, N \tag{9}$$

and for each layer is valid the Eq. (7), so $T^k_t = \theta^k_t$ and $T^k_b = \theta^k_b$, with $k = 1, \ldots, N_l$ and $t = top$ and $b = bottom$. A detailed description of the temperature profile is given in Figure 2 for the three proposed benchmarks.

GEOMETRICAL RELATIONS

Shells and plates are bi-dimensional structures where one dimension, in general the thickness in z direction, is neglected respect to the others two in the plane. Shells have curvature along the in-plane directions, in this paper only shells with constant radii of curvature are considered. Geometry and reference systems for shells are indicated in Figure 1.

For a shell, the square of an infinitesimal linear segment in the layer, the associated infinitesimal area and volume elements are given by:

$$\begin{aligned} ds^2_k &= H^{k^2}_\alpha d\alpha^2_k + H^{k^2}_\beta d\beta^2_k + H^{k^2}_z dz^2_k \\ d\Omega_k &= H^k_\alpha H^k_\beta \, d\alpha_k d\beta_k \\ dV_k &= H^k_\alpha H^k_\beta H^k_z d\alpha_k d\beta_k dz_k \end{aligned} \tag{10}$$

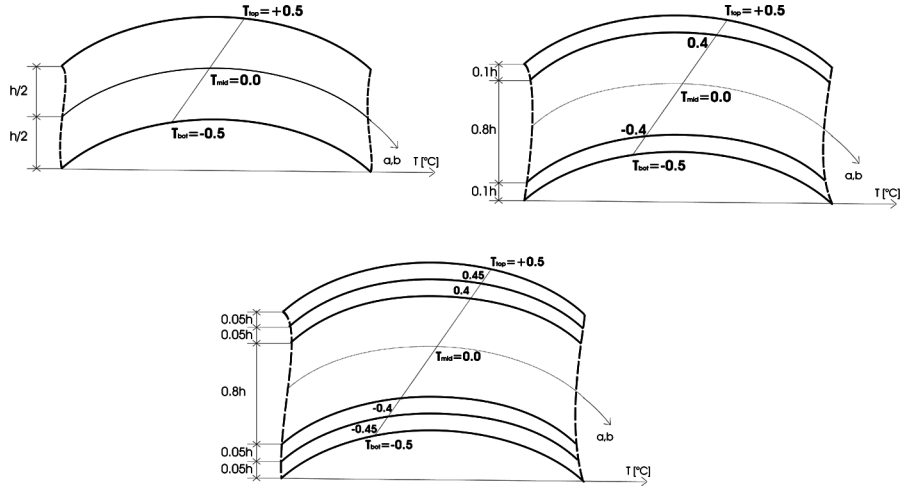

Figure 2 Linear profile of temperature through the thickness for the cylindrical shell (0°/90°), the spherical shell (0°/*core*/0°) and the spherical shell (0°/90°/*core*/90°/0°).

where the metric coefficients are:

$$H_\alpha^k = A^k(1 + z_k/R_\alpha^k), \quad H_\beta^k = B^k(1 + z_k/R_\beta^k), \quad H_z^k = 1 \tag{11}$$

k denotes the kth-layer of the multilayered shell; R_α^k and R_β^k are the principal radii of curvature along the coordinates α_k and β_k respectively. A^k and B^k are the coefficients of the first fundamental form of Ω_k (Γ_k is the Ω_k boundary) [30]. In this paper, the attention has been restricted to shells with constant radii of curvature ($A = B = 1$ for each layer of k).

Given a kth-layer, the geometrical relations permit to express the in-plane $\boldsymbol{\epsilon}_p$ and out-plane $\boldsymbol{\epsilon}_n$ strains in terms of displacement $\boldsymbol{u}$. The following relations hold in the case of a shell:

$$\boldsymbol{\epsilon}_{pG} = [\epsilon_{\alpha\alpha}, \epsilon_{\beta\beta}, \epsilon_{\alpha\beta}]^T = (\boldsymbol{D}_p + \boldsymbol{A}_p)\boldsymbol{u}, \quad \boldsymbol{\epsilon}_{nG} = [\epsilon_{\alpha z}, \epsilon_{\beta z}, \epsilon_{zz}]^T = (\boldsymbol{D}_{np} + \boldsymbol{D}_{nz} - \boldsymbol{A}_n)\boldsymbol{u} \tag{12}$$

where $\boldsymbol{u} = (u_\alpha, u_\beta, u_z)$. The explicit form of the introduced arrays follows:

$$\boldsymbol{D}_p = \begin{bmatrix} \frac{\partial_\alpha}{H_\alpha} & 0 & 0 \\ 0 & \frac{\partial_\beta}{H_\beta} & 0 \\ \frac{\partial_\beta}{H_\beta} & \frac{\partial_\alpha}{H_\alpha} & 0 \end{bmatrix}, \quad \boldsymbol{D}_{np} = \begin{bmatrix} 0 & 0 & \frac{\partial_\alpha}{H_\alpha} \\ 0 & 0 & \frac{\partial_\beta}{H_\beta} \\ 0 & 0 & 0 \end{bmatrix}, \quad \boldsymbol{D}_{nz} = \begin{bmatrix} \partial_z & 0 & 0 \\ 0 & \partial_z & 0 \\ 0 & 0 & \partial_z \end{bmatrix}, \tag{13}$$

$$\boldsymbol{A}_p = \begin{bmatrix} 0 & 0 & \frac{1}{H_\alpha R_\alpha} \\ 0 & 0 & \frac{1}{H_\beta R_\beta} \\ 0 & 0 & 0 \end{bmatrix}, \quad \boldsymbol{A}_n = \begin{bmatrix} \frac{1}{H_\alpha R_\alpha} & 0 & 0 \\ 0 & \frac{1}{H_\beta R_\beta} & 0 \\ 0 & 0 & 0 \end{bmatrix} \tag{14}$$

CONSTITUTIVE RELATIONS

The stresses for the thermomechanical problems have two parts, a mechanical part denoted by the subscript d and a thermal one denoted by the subscript t. In order to use the Principle of Virtual Displacements (PVD), the stresses are split into in-plane components $\boldsymbol{\sigma}_p = (\sigma_{\alpha\alpha}, \sigma_{\beta\beta}, \sigma_{\alpha\beta})$ and into out-plane ones $\boldsymbol{\sigma}_n = (\sigma_{\alpha z}, \sigma_{\beta z}, \sigma_{zz})$.

The constitutive equations are given as:

$$\begin{aligned} \boldsymbol{\sigma}_{pC}^k &= \boldsymbol{\sigma}_{pd}^k - \boldsymbol{\sigma}_{pt}^k = \boldsymbol{C}_{pp}^k \boldsymbol{\epsilon}_{pG}^k + \boldsymbol{C}_{pn}^k \boldsymbol{\epsilon}_{nG}^k - \boldsymbol{\lambda}_p^k T^k \\ \boldsymbol{\sigma}_{nC}^k &= \boldsymbol{\sigma}_{nd}^k - \boldsymbol{\sigma}_{nt}^k = \boldsymbol{C}_{np}^k \boldsymbol{\epsilon}_{pG}^k + \boldsymbol{C}_{nn}^k \boldsymbol{\epsilon}_{nG}^k - \boldsymbol{\lambda}_n^k T^k \end{aligned} \tag{15}$$

where subscript C indicates the constitutive equations and G the geometrical ones. The coefficients $\boldsymbol{\lambda}_p^k$ and $\boldsymbol{\lambda}_n^k$ are linked to the coefficients of thermal expansion $\boldsymbol{\alpha}_p^k$ and $\boldsymbol{\alpha}_n^k$ by:

$$\begin{aligned} \boldsymbol{\lambda}_p^k &= \boldsymbol{\lambda}_{pp}^k + \boldsymbol{\lambda}_{pn}^k = \boldsymbol{C}_{pp}^k \boldsymbol{\alpha}_p^k + \boldsymbol{C}_{pn}^k \boldsymbol{\alpha}_n^k \\ \boldsymbol{\lambda}_n^k &= \boldsymbol{\lambda}_{np}^k + \boldsymbol{\lambda}_{nn}^k = \boldsymbol{C}_{np}^k \, \boldsymbol{\alpha}_p^k + \boldsymbol{C}_{nn}^k \, \boldsymbol{\alpha}_n^k \end{aligned} \tag{16}$$

with the elastic coefficients allocated in the following four sub-arrays

$$\boldsymbol{C}_{pp}^{k} = \begin{bmatrix} C_{11}^{k} & C_{12}^{k} & C_{16}^{k} \\ C_{12}^{k} & C_{22}^{k} & C_{26}^{k} \\ C_{16}^{k} & C_{26}^{k} & C_{66}^{k} \end{bmatrix}, \quad \boldsymbol{C}_{pn}^{k} = \begin{bmatrix} 0 & 0 & C_{13}^{k} \\ 0 & 0 & C_{23}^{k} \\ 0 & 0 & C_{36}^{k} \end{bmatrix}$$
$$\boldsymbol{C}_{np}^{k} = \begin{bmatrix} 0 & 0 & 0 \\ 0 & 0 & 0 \\ C_{13}^{k} & C_{23}^{k} & C_{36}^{k} \end{bmatrix}, \quad \boldsymbol{C}_{nn}^{k} = \begin{bmatrix} C_{55}^{k} & C_{45}^{k} & 0 \\ C_{45}^{k} & C_{44}^{k} & 0 \\ 0 & 0 & C_{33}^{k} \end{bmatrix} \tag{17}$$

The thermal expansion coefficients and the coefficients of thermo-mechanical coupling are:

$$\boldsymbol{\alpha}_{p}^{k} = \begin{bmatrix} \alpha_{11}^{k} \\ \alpha_{22}^{k} \\ 0 \end{bmatrix}, \quad \boldsymbol{\alpha}_{n}^{k} = \begin{bmatrix} 0 \\ 0 \\ \alpha_{33}^{k} \end{bmatrix}, \quad \boldsymbol{\lambda}_{pp}^{k} = \begin{bmatrix} \lambda_{pp1}^{k} \\ \lambda_{pp2}^{k} \\ \lambda_{pp3}^{k} \end{bmatrix}$$
$$\boldsymbol{\lambda}_{pn}^{k} = \begin{bmatrix} 0 \\ 0 \\ \lambda_{pn3}^{k} \end{bmatrix}, \quad \boldsymbol{\lambda}_{np}^{k} = \begin{bmatrix} 0 \\ 0 \\ \lambda_{np3}^{k} \end{bmatrix}, \quad \boldsymbol{\lambda}_{nn}^{k} = \begin{bmatrix} \lambda_{nn1}^{k} \\ \lambda_{nn2}^{k} \\ \lambda_{nn3}^{k} \end{bmatrix}. \tag{18}$$
$$\tag{1}$$

GOVERNING EQUATIONS

This section presents the derivation of the governing equations based on the *Principle of Virtual Displacements* (PVD) in case of a multilayered shell subjected to thermal and/or external mechanical loads. A closed form solution will be developed considering particular material and boundary conditions. The procedure permits to obtain the so-called *fundamental nuclei* that are simple matrices representing the basic element from which the stiffness matrices of the whole structure can be computed.

We consider a multi-layered shell with N_l layers. The PVD for the thermo mechanical case reads:

$$\sum_{k=1}^{N_l} \int_{\Omega_k} \int_{A_k} \left\{ \delta \boldsymbol{\epsilon}_{pG}^{k\,T} \boldsymbol{\sigma}_{pC}^{k} + \delta \boldsymbol{\epsilon}_{nG}^{k\,T} \boldsymbol{\sigma}_{nC}^{k} \right\} d\Omega_k dz = \sum_{k=1}^{N_l} \delta L_e^k \tag{19}$$

where Ω_k and A_k are the integration domains in plane (α, β) and z directions, respectively. k indicates the layer and T the transpose of a vector. δL_e^k is the external work for the kth layer. G means geometrical relations and C constitutive ones. $\boldsymbol{\sigma}_{pC}^{k}$ and $\boldsymbol{\sigma}_{nC}^{k}$ contain the mechanical (d) and thermal (t) contributions, so:

$$\sum_{k=1}^{N_l} \int_{\Omega_k} \int_{A_k} \left\{ \delta \boldsymbol{\epsilon}_{pG}^{k\,T} (\boldsymbol{\sigma}_{pd}^{k} - \boldsymbol{\sigma}_{pt}^{k}) + \delta \boldsymbol{\epsilon}_{nG}^{k\,T} (\boldsymbol{\sigma}_{nd}^{k} - \boldsymbol{\sigma}_{nt}^{k}) \right\} d\Omega_k dz = \sum_{k=1}^{N_l} \delta L_e^k \tag{20}$$

The steps to obtain the governing equations are:

- substitution of geometrical relations (subscript G),

- substitution of appropriate constitutive equations (subscript C),
- introduction of the CUF.

Substituting the geometrical relations Eqs. (12) and constitutive equations Eqs. (15) into the variational statement Eq. (20), we obtain for the kth layer:

$$\int_{\Omega_k}\int_{A_k}\Big[\Big(\big(\boldsymbol{D}_p^k+\boldsymbol{A}_p^k\big)\delta\boldsymbol{u}^k\Big)^T\Big(\boldsymbol{C}_{pp}^k\big(\boldsymbol{D}_p^k+\boldsymbol{A}_p^k\big)\boldsymbol{u}^k+\boldsymbol{C}_{pn}^k\big(\boldsymbol{D}_{np}^k+\boldsymbol{D}_{nz}^k-\boldsymbol{A}_n^k\big)\boldsymbol{u}^k-\boldsymbol{\lambda}_p^kT^k\Big)$$
$$+\Big(\big(\boldsymbol{D}_{np}^k+\boldsymbol{D}_{nz}^k-\boldsymbol{A}_n^k\big)\delta\boldsymbol{u}^k\Big)^T\Big(\boldsymbol{C}_{np}^k\big(\boldsymbol{D}_p^k+\boldsymbol{A}_p^k\big)\boldsymbol{u}^k$$
$$+\boldsymbol{C}_{nn}^k\big(\boldsymbol{D}_{np}^k+\boldsymbol{D}_{nz}^k-\boldsymbol{A}_n^k\big)\boldsymbol{u}^k-\boldsymbol{\lambda}_n^kT^k\Big)\Big]d\Omega_k dz=\delta L_e^k \tag{21}$$

Substituting the CUF, Eqs. (1) and Eq. (9), yielding:

$$\int_{\Omega_k}\int_{A_k}\Big[\Big(\big(\boldsymbol{D}_p^k+\boldsymbol{A}_p^k\big)\ F_s\delta\boldsymbol{u}_s^k\Big)^T\Big(\boldsymbol{C}_{pp}^k\big(\boldsymbol{D}_p^k+\boldsymbol{A}_p^k\big)F_\tau\boldsymbol{u}_\tau^k+\boldsymbol{C}_{pn}^k\big(\boldsymbol{D}_{np}^k+\boldsymbol{D}_{nz}^k-\boldsymbol{A}_n^k\big)F_\tau\boldsymbol{u}_\tau^k-\boldsymbol{\lambda}_p^kF_\tau\theta_\tau^k\Big)$$
$$+\Big(\big(\boldsymbol{D}_{np}^k+\boldsymbol{D}_{nz}^k-\boldsymbol{A}_n^k\big)F_s\delta\boldsymbol{u}_s^k\Big)^T\Big(\boldsymbol{C}_{np}^k\big(\boldsymbol{D}_p^k+\boldsymbol{A}_p^k\big)F_\tau\boldsymbol{u}_\tau^k$$
$$+\boldsymbol{C}_{nn}^k\big(\boldsymbol{D}_{np}^k+\boldsymbol{D}_{nz}^k-\boldsymbol{A}_n^k\big)F_\tau\boldsymbol{u}_\tau^k-\boldsymbol{\lambda}_n^kF_\tau\theta_\tau^k\Big)\Big]d\Omega_k dz=\delta L_e^k \tag{22}$$

After integration by parts, the governing differential equations on domain Ω_k and boundary conditions on edge Γ_k are obtained. Further details on the procedure of integration by parts are reported in [22].

The governing equations for a multi-layered shell subjected to thermal and mechanical loadings are:

$$\delta\boldsymbol{u}_s^{kT}:\boldsymbol{K}_{uu}^{k\tau s}\boldsymbol{u}_\tau^k=-\boldsymbol{K}_{u\theta}^{k\tau s}\boldsymbol{\theta}_\tau^k+\boldsymbol{P}_{u\tau}^k \tag{23}$$

with related boundary conditions on edge Γ_k:

$$\boldsymbol{\Pi}_d^{k\tau s}\boldsymbol{u}_\tau^k-\boldsymbol{\Pi}_t^{k\tau s}\theta_\tau^k=\boldsymbol{\Pi}_d^{k\tau s}\bar{\boldsymbol{u}}_\tau^k-\boldsymbol{\Pi}_t^{k\tau s}\bar{\theta}_\tau^k \tag{24}$$

where $(-\boldsymbol{K}_{u\theta}^{k\tau s}\boldsymbol{\theta}_\tau^k)$ is the thermal load and $\boldsymbol{P}_{u\tau}^k$ is the external mechanical one. The fundamental nuclei $\boldsymbol{K}_{uu}^{k\tau s}$ and $\boldsymbol{K}_{u\theta}^{k\tau s}$ have to be assembled by expanding the indices as described in the following: via τ and s we consider the expansion in z for the considered variables, and via k the assembling on the number of layers is accomplished.

Considering the Eq. (10), the fundamental nuclei are:

$$\boldsymbol{K}_{uu}^{k\tau s}=\int_{A_k}\Big[\big(-\boldsymbol{D}_p^k+\boldsymbol{A}_p^k\big)^T\Big(\boldsymbol{C}_{pp}^k\big(\boldsymbol{D}_p^k+\boldsymbol{A}_p^k\big)\ +\boldsymbol{C}_{pn}^k\big(\boldsymbol{D}_{np}^k+\boldsymbol{D}_{nz}^k-\boldsymbol{A}_n^k\big)\Big)$$
$$+\big(-\boldsymbol{D}_{np}^k+\boldsymbol{D}_{nz}^k-\boldsymbol{A}_n^k\big)^T\Big(\boldsymbol{C}_{np}^k\big(\boldsymbol{D}_p^k+\boldsymbol{A}_p^k\big)+\boldsymbol{C}_{nn}^k\big(\boldsymbol{D}_{np}^k+\boldsymbol{D}_{nz}^k-\boldsymbol{A}_n^k\big)\Big)\Big]F_sF_\tau H_\alpha^kH_\beta^kdz \tag{25}$$

$$\boldsymbol{K}_{u\theta}^{k\tau s}=\int_{A_k}\Big[\big(-\boldsymbol{D}_p^k+\boldsymbol{A}_p^k\big)^T\big(-\boldsymbol{\lambda}_p^k\big)+\big(-\boldsymbol{D}_{np}^k+\boldsymbol{D}_{nz}^k-\boldsymbol{A}_n^k\big)^T\big(-\boldsymbol{\lambda}_n^k\big)\Big]F_sF_\tau H_\alpha^kH_\beta^kdz \tag{26}$$

$$\Pi_d^{k\tau s} = \int_{A_k} \Big[\boldsymbol{I}_p^{kT} \Big(\boldsymbol{C}_{pp}^k \big(\boldsymbol{D}_p^k + \boldsymbol{A}_p^k \big) + \boldsymbol{C}_{pn}^k \big(\boldsymbol{D}_{np}^k + \boldsymbol{D}_{nz}^k - \boldsymbol{A}_n^k \big) \Big) + \boldsymbol{I}_{np}^{kT} \Big(\boldsymbol{C}_{np}^k \big(\boldsymbol{D}_p^k + \boldsymbol{A}_p^k \big) + \boldsymbol{C}_{nn}^k \big(\boldsymbol{D}_{np}^k + \boldsymbol{D}_{nz}^k - \boldsymbol{A}_n^k \big) \Big) \Big] F_s F_\tau H_\alpha^k H_\beta^k dz \tag{27}$$

$$\Pi_t^{k\tau s} = \int_{A_k} \Big[\boldsymbol{I}_p^{kT} \big(-\boldsymbol{\lambda}_p^k \big) + \boldsymbol{I}_{np}^{kT} \big(-\boldsymbol{\lambda}_n^k \big) \Big] F_s F_\tau H_\alpha^k H_\beta^k dz \tag{28}$$

with

$$\boldsymbol{I}_p^k = \begin{bmatrix} \frac{1}{H_\alpha^k} & 0 & 0 \\ 0 & \frac{1}{H_\beta^k} & 0 \\ \frac{1}{H_\beta^k} & \frac{1}{H_\alpha^k} & 0 \end{bmatrix}, \quad \boldsymbol{I}_{np}^k = \begin{bmatrix} 0 & 0 & \frac{1}{H_\alpha^k} \\ 0 & 0 & \frac{1}{H_\beta^k} \\ 0 & 0 & 0 \end{bmatrix} \tag{29}$$

Closed Form Solutions

A Navier-type closed form solution is obtained via substitution of harmonic expressions for the displacements and temperature as well as considering the following coefficients equal to zero: $C_{16} = C_{26} = C_{36} = C_{45} = 0$ and $\lambda_{pp3} = \lambda_{pn3} = 0$.

The following harmonic assumptions can be made for the field variables, that correspond to simply supported boundary conditions:

$$\begin{aligned} u_{\alpha_\tau}^k &= \sum_{m,n} (\widehat{U}_{\alpha_\tau}^k) \cos\left(\frac{m\pi\alpha_k}{a_k}\right) \sin\left(\frac{n\pi\beta_k}{b_k}\right) \quad k = 1, N_l \\ u_{\beta_\tau}^k &= \sum_{m,n} (\widehat{U}_{\beta_\tau}^k) \sin\left(\frac{m\pi\alpha_k}{a_k}\right) \cos\left(\frac{n\pi\beta_k}{b_k}\right) \quad \tau = t, b, r \\ u_{z_\tau}^k &= \sum_{m,n} (\widehat{U}_{z_\tau}^k) \sin\left(\frac{m\pi\alpha_k}{a_k}\right) \sin\left(\frac{n\pi\beta_k}{b_k}\right) \quad r = 2, N \\ \theta_\tau^k &= \sum_{m,n} (\hat{\theta}_\tau^k) \sin\left(\frac{m\pi\alpha_k}{a_k}\right) \sin\left(\frac{n\pi\beta_k}{b_k}\right) \end{aligned} \tag{30}$$

where $\widehat{U}_{\alpha_\tau}^k$, $\widehat{U}_{\beta_\tau}^k$, $\widehat{U}_{z_\tau}^k$ and $\hat{\theta}_\tau^k$ are the amplitudes, m and n the wave numbers, and a_k and b_k the shell dimensions.

The explicit forms of the fundamental nuclei $\boldsymbol{K}_{uu}^{k\tau s}(3 \times 3)$ and $\boldsymbol{K}_{u\theta}^{k\tau s}(3 \times 1)$ are given in the Appendix.

RESULTS AND DISCUSSION

Here, three different benchmarks are discussed, these all have been provided by Khare et al. [6]. The first is a cylindrical shell made of two carbon fiber reinforced layers with cross-ply orientation (0°/90°). The second and third case consist of spherical shell with a central soft core and external carbon fiber reinforced layers; the case two has two external layers with the same orientation 0°, while in the case three the soft core links two layers at the top with orientation (90°/0°) and

Table 1 Cylindrical shell: geometry and materials properties

E_1/E_2	25
$E_2 = E_3$	
G_{12}/G_{23}	2.5
$G_{12} = G_{13}$	
$\nu_{12} = \nu_{13} = \nu_{23}$	0.25
α_{22}/α_{11}	3
$\alpha_{11} = \alpha_{33}$ [/°C]	
$a = b$ [m]	1
h [m]	0.1
$h_{0°} = h_{90°}[m]$	0.05
R_α [m]	∞
R_β [m]	5, 10, 50

two layers at the bottom with orientation (0°/90°). The notation for the geometry and the curvilinear reference system for shells with constant radii of curvature are indicated in Figure 1. Geometry and materials properties for the cylindrical shell are indicated in Table 1. Table 2 contains the data for the two considered spherical shells. The applied thermal load is due to a temperature distribution that varies in

Table 2 Spherical shell: geometry and materials properties

Faces	
E_1 [GPa]	172.37
$E_2 = E_3$ [GPa]	6.89
$G_{12} = G_{13}$ [GPa]	3.45
G_{23} [GPa]	1.38
$\nu_{12} = \nu_{13} = \nu_{23}$	0.25
α_{22} [10^{-5}/°C]	2
$\alpha_{11} = \alpha_{33}$ [10^{-5}/°C]	0.1
Core	
$E_1 = E_2$ [GPa]	0.28
E_3 [GPa]	3.45
G_{12} [GPa]	0.11
$G_{13} = G_{23}$ [GPa]	0.41
$\nu_{12} = \nu_{13} = \nu_{23}$	0.02
α_{22} [10^{-5}/°C]	0.2
$\alpha_{11} = \alpha_{33}$ [10^{-6}/°C]	0.1
Geometry	
$a = b$ [m]	1
h [m]	0.25, 0.01
h_c [m]	0.8 h
$h_f(0°/c/0°)$ [m]	0.1 h
$h_f(0°/90°/c/90°/0°)$ [m]	0.05 h
$R_\alpha = R_\beta$ [m]	5, 10, 20

Table 3 Linear through the thickness thermal load

R/a	5	10	50
HOST12[6]	1.1261	1.1434	1.1493
HSDT[7]	1.1235	1.1421	1.1482
ESL theories			
CLT	1.1834	1.1966	1.1997
FSDT	1.1805	1.1959	1.1997
ED1	1.1806	1.1959	1.1997
ED2	1.1255	1.1411	1.1455
ED3	1.1264	1.1422	1.1466
ED4	1.1276	1.1434	1.1479
Zig-zag theories			
EDZ1	1.1203	1.1361	1.1406
EDZ2	1.1260	1.1416	1.1460
EDZ3	1.1259	1.1416	1.1460

Cylindrical shell (0°/90°) with thickness ratio $a/h = 10$. Equivalent Single Layer theories. Transverse displacement $\bar{u}_z = \frac{u_z(a/2,b/2,0)}{\alpha_1 T_1 b^2}$.

a bi-sinusoidal form in-the-plane and linear in the thickness direction:

$$\Delta T = \left(T_0 + \frac{z}{h}T_1\right) \sin\left(\frac{m\pi}{a}\alpha\right) \sin\left(\frac{n\pi}{b}\beta\right) \tag{31}$$

Khare et al. [6] considers a zero mean value of temperature ($T_0 = 0$) and a gradient T_1 equal to 1. In this way the values of temperature at the top and at the bottom are $T_t = 0.5$ and $T_b = -0.5$, respectively. All the data are given for a correspondent environmental temperature which is a free parameter. In the present ESL and LW models, the assigned linear distribution of temperature will be considered always LW. The distribution of temperature is always assigned as in Figure 2, to compare the proposed refined models with those presented in [6] and [7].

Table 4 Linear through the thickness thermal load

R/a	5	10	50
ED4	1.1276	1.1434	1.1479
LW theories			
LD1	1.1425	1.1577	1.1620
LD2	1.1262	1.1414	1.1457
LD3	1.1280	1.1434	1.1477
LD4	1.1280	1.1434	1.1477

Cylindrical shell (0°/90°) with thickness ratio $a/h = 10$. Layer-Wise theories. Transverse displacement $\bar{u}_z = \frac{u_z(a/2,b/2,0)}{\alpha_1 T_1 b^2}$.

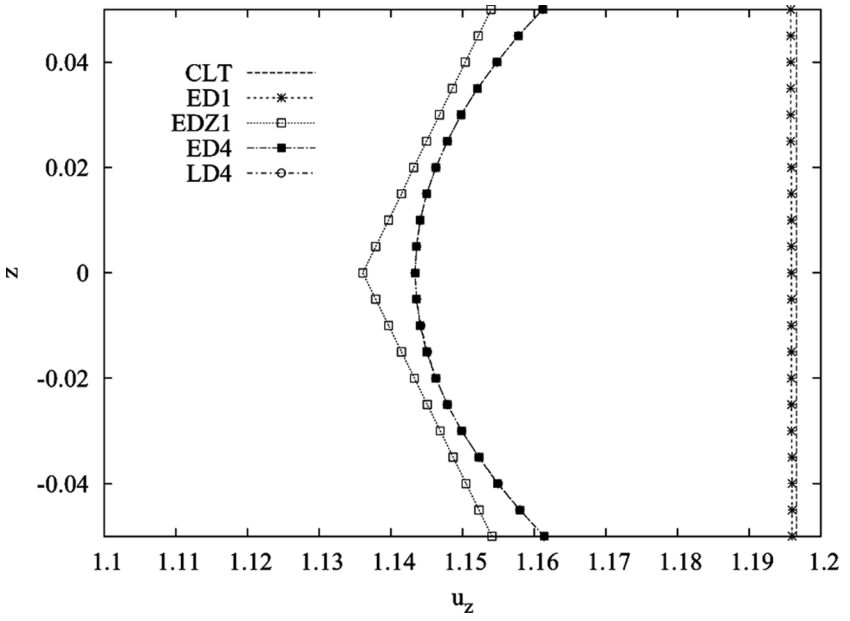

Figure 3 Cylindrical shell (0°/90°) with radius of curvature $R_\beta/a = 10$. Non-dimensional transverse displacement $\bar{u}_z$ through the thickness z. Thickness ratio $a/h = 10$.

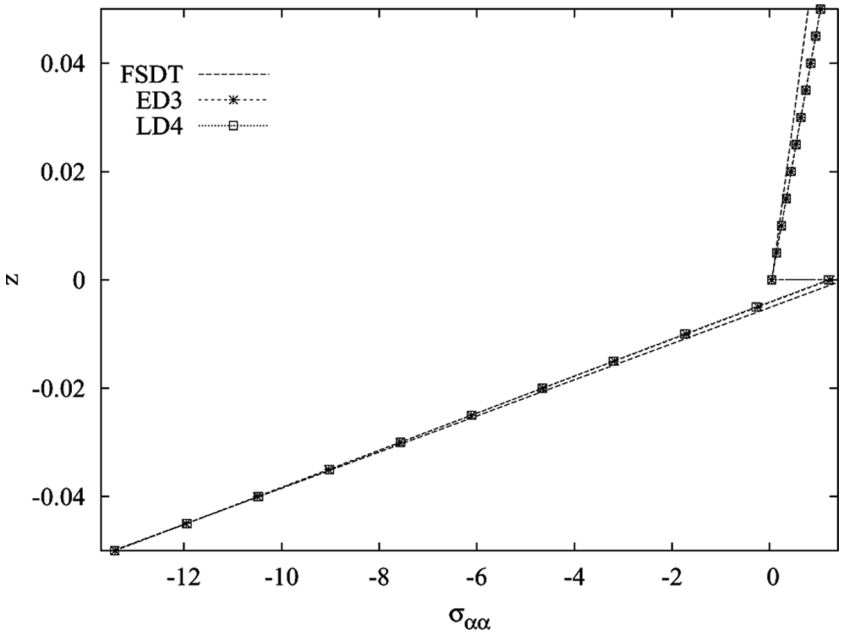

Figure 4 Cylindrical shell (0°/90°) with radius of curvature $R_\beta/a = 10$. In-plane stress σ_{zz} through the thickness z. Thickness ratio $a/h = 10$.

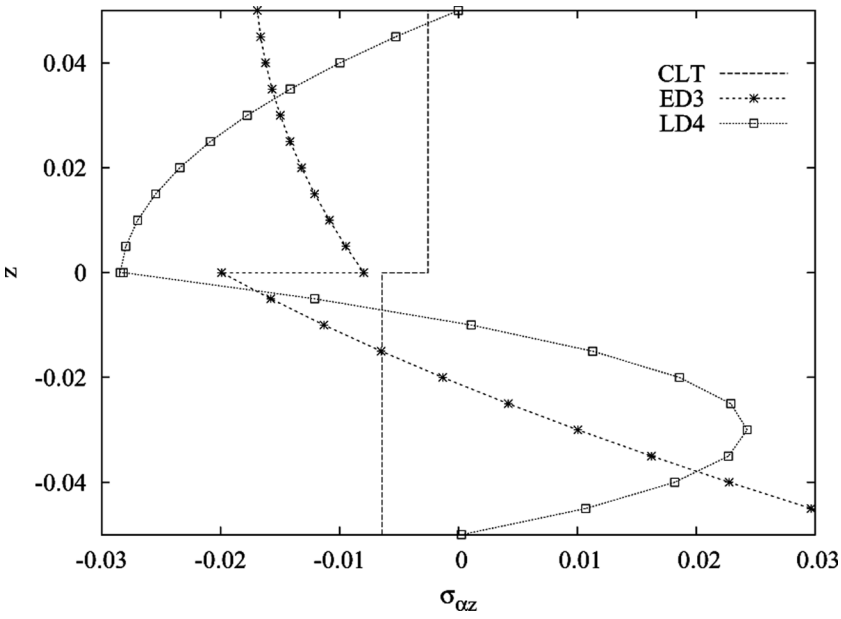

Figure 5 Cylindrical shell (0°/90°) with radius of curvature $R_\beta/a = 10$. Transverse shear stress $\sigma_{\alpha z}$ through the thickness z. Thickness ratio $a/h = 10$.

Table 5 Linear through the thickness thermal load

	$a/h = 4$				$a/h = 100$			
R/a	5	10	20	Plate	5	10	20	Plate
HOST12[6]	4.2032	4.2343	4.2422	4.2448	0.8780	1.4368	1.7077	1.8221
FOST[6]	3.2618	3.2745	3.2775	3.2784	0.8624	1.4085	1.6726	1.7840
ESL theories								
CLT	1.8043	1.8025	1.8021	1.8019	0.8750	1.4256	1.6904	1.8019
FSDT	3.1472	3.1632	3.1672	3.1685	0.8738	1.4264	1.6931	1.8055
ED1	3.1466	3.1631	3.1672	3.1685	0.8781	1.4293	1.6941	1.8055
ED2	3.0306	3.0471	3.0512	3.0525	0.8764	1.4343	1.7045	1.8185
ED3	4.1867	4.2308	4.2419	4.2456	0.8789	1.4383	1.7092	1.8235
ED4	4.1928	4.2360	4.2469	4.2505	0.8658	1.4178	1.6853	1.7983
Zig-zag theories								
EDZ1	4.3705	4.4190	4.4312	4.4352	0.8822	1.4347	1.6997	1.8112
EDZ2	4.3228	4.3720	4.3843	4.3885	0.8800	1.4395	1.7102	1.8244
EDZ3	4.3261	4.3754	4.3878	4.3919	0.8800	1.4395	1.7102	1.8244

Spherical shell (0°/*core*/0°) with thickness ratio $a/h = 4$ and $a/h = 100$. Equivalent Single Layer theories. Transverse displacement $\bar{u}_z = \frac{10hu_z(a/2,b/2,0)}{\alpha_1 T_1 a^2}$.

Table 6 Linear through the thickness thermal load

	$a/h = 4$				$a/h = 100$			
R/a	5	10	20	Plate	5	10	20	Plate
ED4	4.1928	4.2360	4.2469	4.2505	0.8658	1.4178	1.6853	1.7983
LW theories								
LD1	4.3417	4.3653	4.3712	4.3732	0.8640	1.4122	1.6779	1.7901
LD2	4.3420	4.3651	4.3709	4.3729	0.8637	1.4118	1.6774	1.7896
LD3	4.3427	4.3658	4.3716	4.3736	0.8637	1.4118	1.6774	1.7896
LD4	4.3426	4.3657	4.3715	4.3735	0.8637	1.4118	1.6774	1.7896

Spherical shell $(0°/core/0°)$ with thickness ratio $a/h = 4$ and $a/h = 100$. Layer Wise theories. Transverse displacement $\bar{u}_z = \frac{10hu_z(a/2,b/2,0)}{\alpha_1 T_1 a^2}$.

Table 7 Linear through the thickness thermal load

R/a	5	10	20	Plate
HOST12[6]	1.7738	1.7915	1.7959	1.7974
FOST[6]	1.7771	1.7768	1.7893	1.7901
ESL theories				
CLT	1.8031	1.8022	1.8020	1.8019
FSDT	1.7988	1.8087	1.8111	1.8120
ED1	1.7984	1.8086	1.8111	1.8120
ED2	1.6523	1.6624	1.6649	1.6658
ED3	1.7700	1.7902	1.7952	1.7969
ED4	1.8125	1.8321	1.8370	1.8386
Zig-zag theories				
EDZ1	1.7976	1.8091	1.8120	1.8129
EDZ2	1.6602	1.6718	1.6747	1.6756
EDZ3	1.7642	1.7845	1.7897	1.7914

Spherical shell $(0°/90°/core/90°/0°)$ with thickness ratio $a/h = 4$. Equivalent Single Layer theories. Transverse displacement $\bar{u}_z = \frac{10hu_z(a/2,b/2,0)}{\alpha_1 T_1 a^2}$.

Table 8 Linear through the thickness thermal load

R/a	5	10	20	Plate
ED4	1.8125	1.8321	1.8370	1.8386
LW theories				
LD1	1.8046	1.8206	1.8246	1.8260
LD2	1.8060	1.8220	1.8260	1.8273
LD3	1.8059	1.8219	1.8260	1.8273
LD4	1.8059	1.8219	1.8259	1.8273

Spherical shell $(0°/90°/core/90°/0°)$ with thickness ratio $a/h = 4$. Layer Wise theories. Transverse displacement $\bar{u}_z = \frac{10hu_z(a/2,b/2,0)}{\alpha_1 T_1 a^2}$.

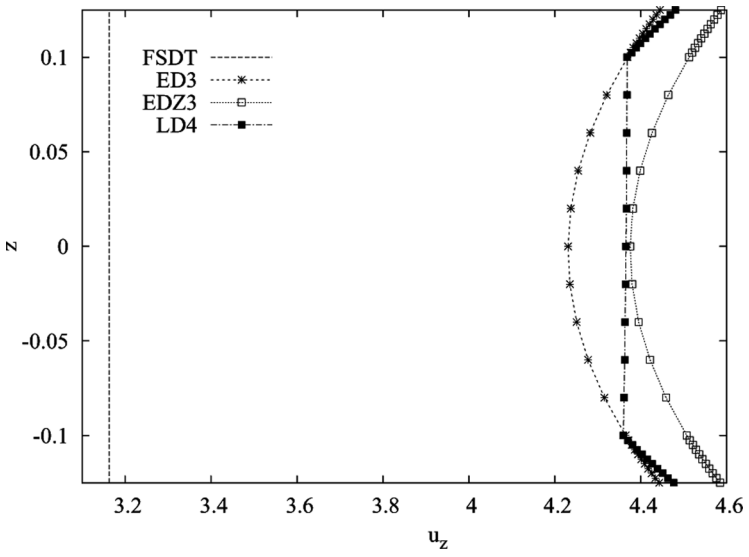

Figure 6 Spherical shell (0°/*core*/0°) with radius of curvature $R_\beta/a = 10$. Non-dimensional transverse displacement $\bar{u}_z$ through the thickness z. Thickness ratio $a/h = 4$.

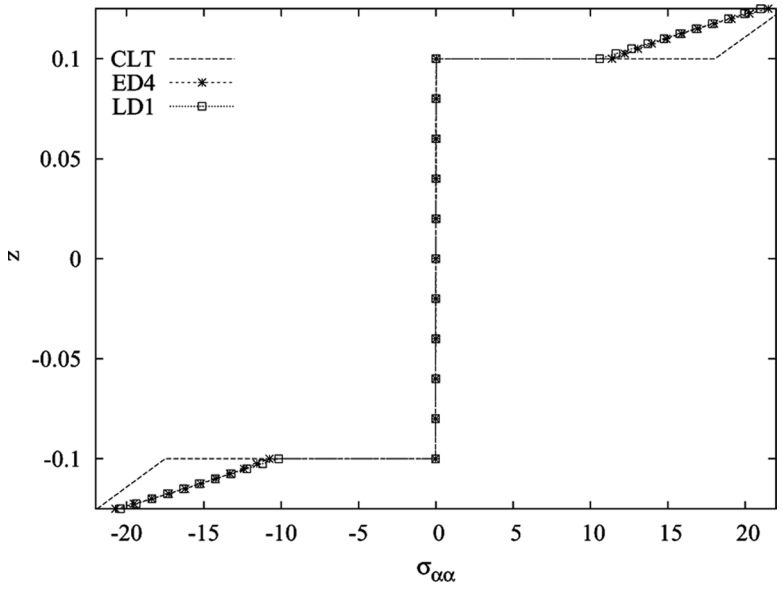

Figure 7 Spherical shell (0°/*core*/0°) with radius of curvature $R_\beta/a = 10$. In-plane stress $\sigma_{\alpha\alpha}$ through the thickness z. Thickness ratio $a/h = 4$.

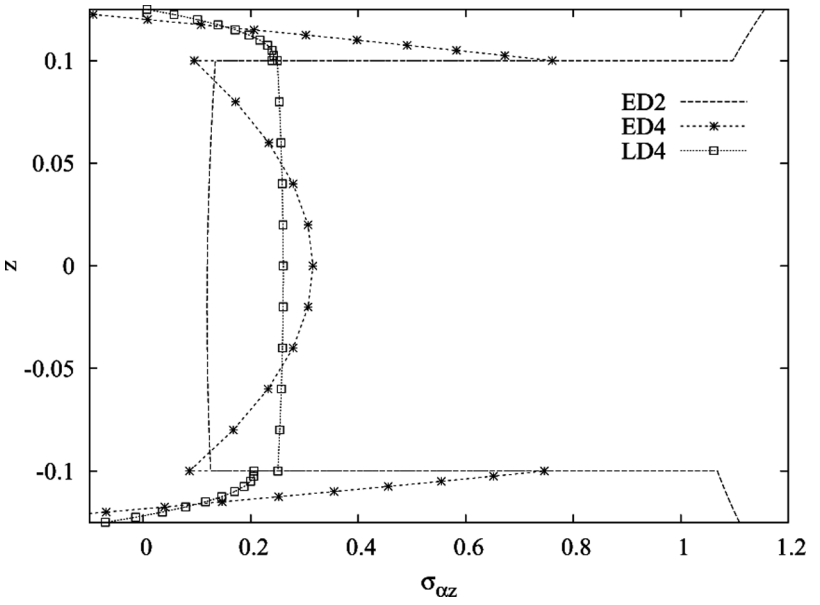

Figure 8 Spherical shell (0°/*core*/0°) with radius of curvature $R_\beta/a = 10$. Transverse shear stress $\sigma_{\alpha z}$ through the thickness z. Thickness ratio $a/h = 4$.

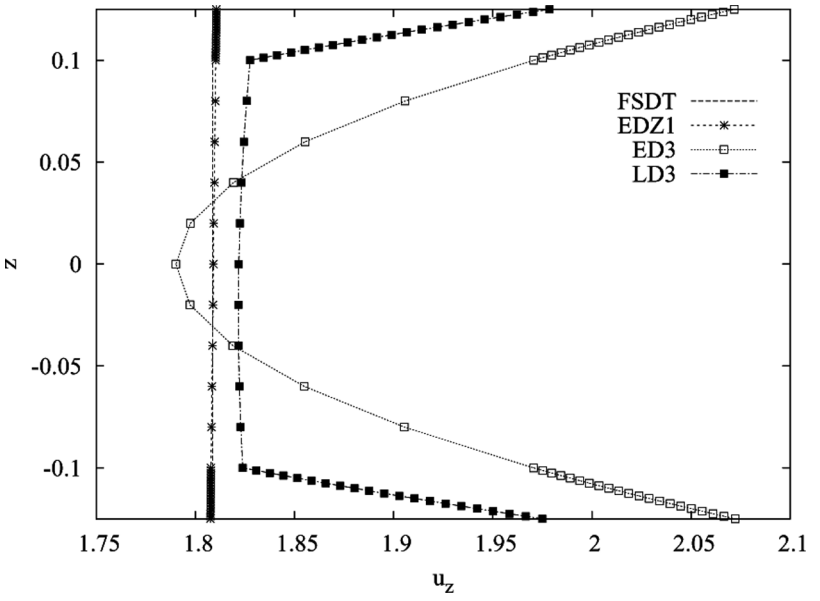

Figure 9 Spherical shell (0°/90°/*core*/90°/0°) with radius of curvature $R_\beta/a = 10$. Non-dimensional transverse displacement $\bar{u}_z$ through the thickness z. Thickness ratio $a/h = 4$.

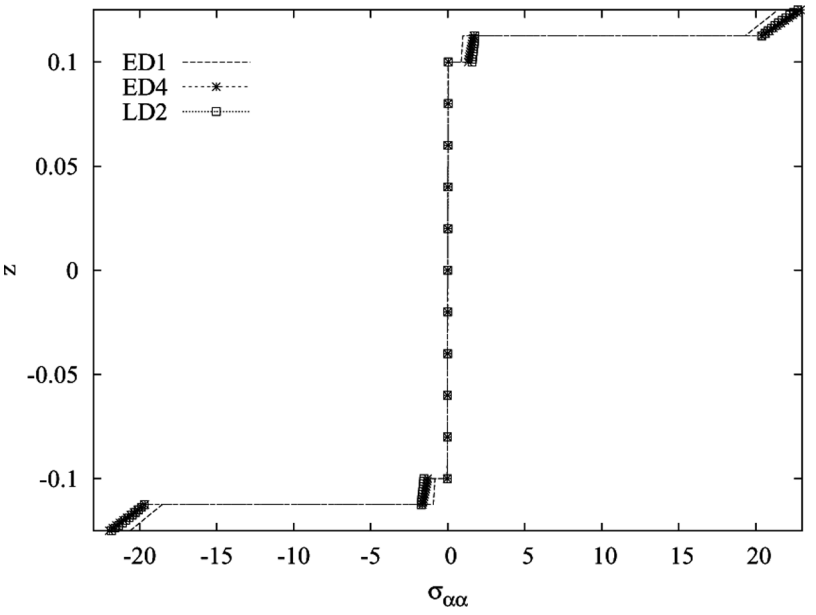

Figure 10 Spherical shell (0°/90°/*core*/90°/0°) with radius of curvature $R_\beta/a = 10$. In-plane stress $\sigma_{\alpha\alpha}$ through the thickness z. Thickness ratio $a/h = 4$.

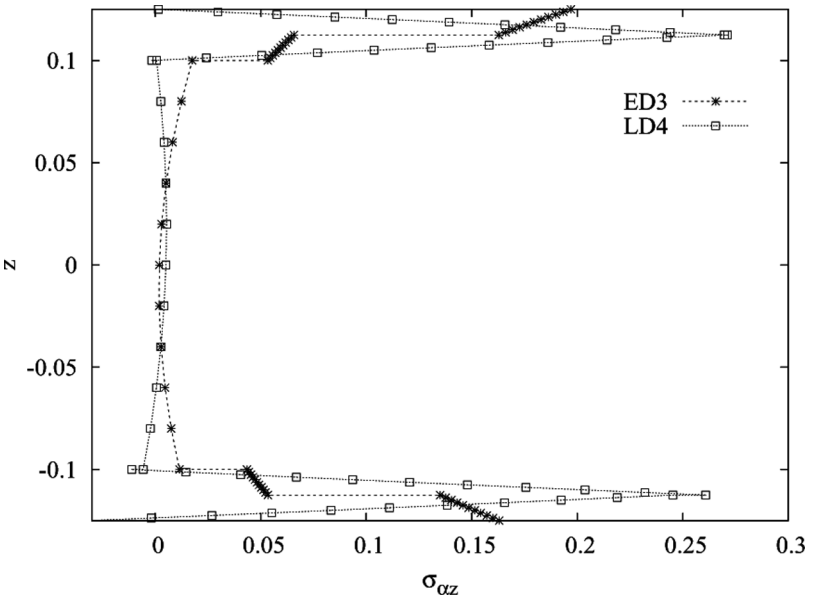

Figure 11 Spherical shell (0°/90°/*core*/90°/0°) with radius of curvature $R_\beta/a = 10$. Transverse shear stress $\sigma_{\alpha z}$ through the thickness z. Thickness ratio $a/h = 4$.

The two models proposed in [6] consist of an equivalent single layer model with cubic expansion in the z direction for the three displacement components (named HOST12), and a first order shear deformation theory (called FOST). Khdeir et al. [7] proposed an higher order shear deformation theory (HSDT) for the benchmark one.

Tables 3 and 4 consider the non-dimensional transverse displacement of the middle surface for the two-layered cylindrical shell. The present ESL models are compared with the HOST12 [6] and the HSDT [7] in Table 3. Third- or fourth-order of expansion (ED3 and ED4) are in good agreement with HOST12 and HSDT; low order of expansion in the thickness direction and classical models such as CLT and FSDT give an error larger than the 5% with respect to the ED4. The effect of the zig-zag Murakami's function is also investigated in Table 3. Significant improvements are outlined for the ED1 with the use of the zig-zag function (denoted as EDZ1): the error for the EDZ1 with respect to the ED4 is less than 1%. Finally, the layer-wise analysis is reported in Table 4: if only the value of displacement in the middle is investigated, there are no significant improvements with respect to the ED4 (higher order of expansion); however the importance of LW models is clearly shown in Figures 3–5, in particular for the transverse shear stress σ_{xz}. Each stress considered in the figures has only the mechanical part (d). Tables 5–8 deal with for the spherical shell with lamination $0°/core/0°$ and $0°/90°/core/90°/0°$, respectively. The importance of layer wise models is evident in these tables and confirmed in the Figures 6–11. The benchmark $0°/core/0°$ shows an important difference between LD4 and ED4; such a difference is negligible in the benchmark $0°/90°/core/90°/0°$, due to the fact that the transverse displacement is considered in the middle of the core with very stiff faces. In this last benchmark there are two important considerations: -for low order of expansion the LW models work better than the ESL ones, -LW models are mandatory to obtain a correct evaluation of the variables along the whole thickness direction (for example in Figure 9 the displacement is quite similar in the middle of the shell for all the considered theories, but these differences increase near the top and the bottom of the considered multilayer). The effect of the curvature R/a has been investigated in each table, no remarkable differences have been found. The effect of the thickness ratio a/h is further illustrated in Tables 5 and 6. Conclusions already known for the plate geometries are confirmed.

CONCLUSIONS

This paper has investigated the thermal bending of multilayered composite shells with constant radii of curvature. The effect of variable kinematics (ESL vs LW models, and higher-order vs lower-order of expansion) has been investigated. It has been mainly concluded that the use of refined models (higher order of expansion in the thickness direction) is mandatory in the thermal response of multilayered composite shells. Layer-wise models are required to describe the transverse variables such as the transverse shear/normal stresses through the whole shell thickness direction.

REFERENCES

1. L. Librescu and P. Marzocca, *Thermal Stresses'03*, vol. 1, Virginia Polytechnic Institute and State University, Blacksburg, VA (USA), 2003.
2. L. Librescu and P. Marzocca, *Thermal Stresses'03*, vol. 2, Virginia Polytechnic Institute and State University, Blacksburg, VA (USA), 2003.
3. A. K. Noor and W. S. Burton, Computational Models for High-Temperature Multilayered Composite Plates and Shells, *Applied Mechanics Reviews*, vol. 45, no. 10, pp. 419–446, 1992.
4. Wu Zhen and Chen Wanji, A Global-Local Higher Order Theory for Multilayered Shells and the Analysis of Laminated Cylindrical Shell Panels, *Comp. Struct.*, vol. 84, no. 4, pp. 350—361, 2008.
5. R. Rolfes, J. Noack, and M. Taeschner, High Performance 3D-Analysis of Thermo-Mechanically Loaded Composite Structures, *Comp. Struct.*, vol. 46, no. 4, pp. 367–379, 1999.
6. R. K. Khare, T. Kant, and A. K. Garg, Closed-Form Thermo-Mechanical Solutions of Higher-Order Theories of Cross-Ply Laminated Shallow Shells, *Comp. Struct.*, vol. 59, no. 3, pp. 313–340, 2003.
7. A. A. Khdeir, M. D. Rajab, and J. N. Reddy, Thermal Effects on the Response of Cross-Ply Laminated Shallow Shells, *Inter. J. Solids Struct.*, vol. 29, no. 5, pp. 653–667, 1992.
8. A. A. Khdeir, Thermoelastic Analysis of Cross-Ply Laminated Circular Cylindrical Shells, *Inter. J. Solids Struct.*, vol. 33, no. 27, pp. 4007–4017, 1996.
9. M. Birsan, Thermal Stresses in Cylindrical Cosserat Elastic Shells, *Euro. J. Mech. A/Solids*, in press, 2008.
10. D. Iesan, Thermal Stresses in Heterogeneous Anisotropic Cosserat Elastic Cylinders, *J. Thermal Stresses*, vol. 8, no. 4, pp. 385–397, 1985.
11. A. Barut, E. Madenci, and A. Tessler, Nonlinear Thermoelastic Analysis of Composite Panels under Non-uniform Temperature Distribution, *Inter. J. Solids Struct.*, vol. 37, no. 7, pp. 3681–3713, 2000.
12. Y. S. Hsu, J. N. Reddy, and C. W. Bert, Thermoelasticity of Circular Cylindrical Shells Laminated of Bimodulus Composite Materials, *J. Thermal Stresses*, vol. 4, no. 2, pp. 155–177, 1981.
13. K. Ding, Thermal Stresses of Weak Formulation Study for Thick Open Laminated Shell, *J. Thermal Stresses*, vol. 31, no. 4, pp. 389–400, 2008.
14. C. J. Miller, W. A. Millavec, and T. P. Richer, Thermal Stress Analysis of Layered Cylindrical Shells, *AIAA J.*, vol. 19, no. 4, pp. 523–530, 1981.
15. J. Padovan, Thermoelasticity of Cylindrically Anisotropic Generally Laminated Cylinders, *J. Appl. Mech.*, vol. 43, no. 1, pp. 124–130, 1976.
16. P. C. Dumir, J. K. Nath, P. Kumari, and S. Kapuria, Improved Efficient Zigzag and Third Order Theories for Circular Cylindrical Shells under Thermal Loading, *J. Thermal Stresses*, vol. 31, no. 4, pp. 343–367, 2008.
17. S. Kapuria, S. Sengupta, and P. C. Dumir, Three-Dimensional Solution for a Hybrid Cylindrical Shell under Axisymmetric Thermoelectric Load, *Arch. Appl. Mech.*, vol. 67, no. 5, pp. 320–330, 1997.
18. D. Holstein, P. Aswendt, R. Hofling, C.-D. Schmidt, and W. Jiiptner, Deformation Analysis of Thermally Loaded Composite Tubes, *Compo. Struct.*, vol. 40, no. 3–4, pp. 257–265, 1998.
19. E. Carrera, Temperature Profile Influence on Layered Plates Response Considering Classical and Advanced Theories, *AIAA J.*, vol. 40, no. 9, pp. 1885–1896, 2002.

20. E. Carrera, An Assessment of Mixed and Classical Theories for the Thermal Stress Analysis of Orthotropic Multilayered Plates, *J. Thermal Stresses*, vol. 23, no. 9, pp. 797–831, 2000.
21. S. Brischetto, R. Leetsch, E. Carrera, T. Wallmersperger, and B. Kroplin, Thermomechanical Bending of Functionally Graded plates, *J. Thermal Stresses*, vol. 31, no. 3, pp. 286–308, 2008.
22. E. Carrera, A Class of Two Dimensional Theories for Multilayered Plates Analysis, *Atti Accademia delle Scienze di Torino, Mem. Sci. Fis.*, vol. 19–20, pp. 49–87, 1995.
23. L. Librescu and W. Lin, Non-linear Response of Laminated Plates and Shells to Thermomechanical Loading: Implications of Violation of Interlaminar Shear Traction Continuity Requirement, *Inter. J. Solids and Struct.*, vol. 36, pp. 4111–4147, 1999.
24. E. Carrera and S. Brischetto, Analysis of Thickness Locking in Classical, Refined and Mixed Multilayered Plate Theories, *Compo. Struct.*, vol. 82, no. 4, pp. 549–562, 2008.
25. E. Carrera and S. Brischetto, Analysis of Thickness Locking in Classical, Refined and Mixed Theories for Layered Shells, *Compo. Struct.*, vol. 85, no. 1, pp. 83–90, 2008.
26. H. Murakami, Laminated Composite Plates Theory with Improved In-plane Response, *J. Appl. Mech.*, vol. 53, no. 33, pp. 661–666, 1986.
27. E. Carrera, On the Use of Murakami's Zig-zag Function in the Modeling of Layered Plates and Shells, *Comp. Struct.*, vol. 82, no. 7–8, pp. 541–554, 2004.
28. L. Demasi, Refined Multilayered Plate Elements Based on Murakami Zig-zag Functions, *Comp. Struct.*, vol. 70, no. 3, pp. 308–316, 2005.
29. J. N. Reddy, *Mechanics of Laminated Composite Plates and Shells*, CRC Press, Boca Raton, FL (USA), 2004.
30. A. W. Leissa, *Vibration of Shells*, NASA SP-288, 1973, National Aeronautics and Space Administration, Washington, DC.

APPENDIX

The explicit expressions of the fundamental nuclei are listed below for the case of a closed form solution. $\alpha = m\pi/a$ and $\beta = n\pi/b$, with m and n as the wave numbers in in-plane directions and a and b as the shell dimensions.

- K_{uu}

$$K_{uu_{11}} = C_{55}^k J_{\alpha\beta}^{k\tau_z s_z} + \frac{1}{R_\alpha^k} C_{55}^k \left(- J_\beta^{k\tau_z s} - J_\beta^{k\tau s_z} + \frac{1}{R_\alpha^k} J_{\beta/\alpha}^{k\tau s} \right) + C_{11}^k J_{\beta/\alpha}^{k\tau s} \alpha^2 + C_{66}^k J_{\alpha/\beta}^{k\tau s} \beta^2$$

$$K_{uu_{12}} = J^{k\tau s} \alpha\beta (C_{12}^k + C_{66}^k) = K_{uu_{21}}$$

$$K_{uu_{13}} = C_{55}^k \left(J_\beta^{k\tau_z s} \alpha - \frac{1}{R_\alpha^k} J_{\beta/\alpha}^{k\tau s} \alpha \right) - C_{13}^k J_\beta^{k\tau s_z} \alpha - \frac{1}{R_\alpha^k} C_{11}^k J_{\beta/\alpha}^{k\tau s} \alpha - C_{12}^k J^{k\tau s} \alpha \frac{1}{R_\beta^k}$$

$$K_{uu_{22}} = C_{44}^k J_{\alpha\beta}^{k\tau_z s_z} + \frac{1}{R_\beta^k} C_{44}^k \left(- J_\alpha^{k\tau_z s} - J_\alpha^{k\tau s_z} + \frac{1}{R_\beta^k} J_{\alpha/\beta}^{k\tau s} \right) + C_{22}^k J_{\alpha/\beta}^{k\tau s} \beta^2 + C_{66}^k J_{\beta/\alpha}^{k\tau s} \alpha^2$$

$$K_{uu_{23}} = C_{44}^k (J_\alpha^{k\tau_z s} \beta - \frac{1}{R_\beta^k} J_{\alpha/\beta}^{k\tau s} \beta) - C_{23}^k J_\alpha^{k\tau s_z} \beta - \frac{1}{R_\beta^k} C_{22}^k J_{\alpha/\beta}^{k\tau s} \beta - \frac{1}{R_\alpha^k} C_{12}^k J^{k\tau s} \beta$$

$$K_{uu_{31}} = C_{55}^k J_\beta^{k\tau s_z} \alpha - C_{55}^k \frac{1}{R_\alpha^k} J_{\beta/\alpha}^{k\tau s} \alpha - C_{13}^k J_\beta^{k\tau_z s} \alpha - \frac{1}{R_\alpha^k} C_{11}^k J_{\beta/\alpha}^{k\tau s} \alpha - \frac{1}{R_\beta^k} C_{12}^k J^{k\tau s} \alpha$$

$$K_{uu_{32}} = C_{44}^k\left(J_\alpha^{k\tau s_z}\beta - \frac{1}{R_\beta^k}J_{\alpha/\beta}^{k\tau s}\beta\right) - C_{23}^k J_\alpha^{k\tau_z s}\beta - \frac{1}{R_\beta^k}C_{22}^k J_{\alpha/\beta}^{k\tau s}\beta - \frac{1}{R_\alpha^k}C_{12}^k J^{k\tau s}\beta$$

$$K_{uu_{33}} = C_{55}^k J_{\beta/\alpha}^{k\tau s}\alpha^2 + C_{44}^k J_{\alpha/\beta}^{k\tau s}\beta^2 + C_{33}^k J_{\alpha\beta}^{k\tau_z s_z} + \frac{1}{R_\alpha^k}\left(\frac{1}{R_\alpha^k}C_{11}^k J_{\beta/\alpha}^{k\tau s} + C_{13}^k J_\beta^{k\tau s_z} + C_{13}^k J_\beta^{k\tau_z s}\right)$$
$$+ \frac{2}{R_\alpha^k R_\beta^k}J^{k\tau s}C_{12}^k + \frac{1}{R_\beta^k}\left(\frac{1}{R_\beta^k}C_{22}^k J_{\alpha/\beta}^{k\tau s} + C_{23}^k J_\alpha^{k\tau_z s} + C_{23}^k J_\alpha^{k\tau s_z}\right)$$

- $K_{u\theta}$

$$K_{u\theta_1} = \alpha J_\beta^{k\tau s}(\lambda_{pp1}^k + \lambda_{pn1}^k)$$
$$K_{u\theta_2} = \beta J_\alpha^{k\tau s}(\lambda_{pp2}^k + \lambda_{pn2}^k)$$
$$K_{u\theta_3} = -J_\beta^{k\tau s}\frac{1}{R_\alpha^k}(\lambda_{pp1}^k + \lambda_{pn1}^k) - J_\alpha^{k\tau s}\frac{1}{R_\beta^k}(\lambda_{pp2}^k + \lambda_{pn2}^k) - J_{\alpha\beta}^{k\tau_z s}(\lambda_{nn3}^k + \lambda_{np3}^k)$$

The meaning of the integrals in z direction is reported as:

$$\left(J^{k\tau s}, J_\alpha^{k\tau s}, J_\beta^{k\tau s}, J_{\frac{\alpha}{\beta}}^{k\tau s}, J_{\frac{\beta}{\alpha}}^{k\tau s}, J_{\alpha\beta}^{k\tau s}\right) = \int_{A_k} F_\tau F_s\left(1, H_\alpha^k, H_\beta^k, \frac{H_\alpha^k}{H_\beta^k}, \frac{H_\beta^k}{H_\alpha^k}, H_\alpha^k H_\beta^k\right)dz$$

$$\left(J^{k\tau_z s}, J_\alpha^{k\tau_z s}, J_\beta^{k\tau_z s}, J_{\frac{\alpha}{\beta}}^{k\tau_z s}, J_{\frac{\beta}{\alpha}}^{k\tau_z s}, J_{\alpha\beta}^{k\tau_z s}\right) = \int_{A_k} \frac{\partial F_\tau}{\partial z}F_s\left(1, H_\alpha^k, H_\beta^k, \frac{H_\alpha^k}{H_\beta^k}, \frac{H_\beta^k}{H_\alpha^k}, H_\alpha^k H_\beta^k\right)dz$$

$$\left(J^{k\tau s_z}, J_\alpha^{k\tau s_z}, J_\beta^{k\tau s_z}, J_{\frac{\alpha}{\beta}}^{k\tau s_z}, J_{\frac{\beta}{\alpha}}^{k\tau s_z}, J_{\alpha\beta}^{k\tau s_z}\right) = \int_{A_k} F_\tau \frac{\partial F_s}{\partial z}\left(1, H_\alpha^k, H_\beta^k, \frac{H_\alpha^k}{H_\beta^k}, \frac{H_\beta^k}{H_\alpha^k}, H_\alpha^k H_\beta^k\right)dz$$

$$\left(J^{k\tau_z s_z}, J_\alpha^{k\tau_z s_z}, J_\beta^{k\tau_z s_z}, J_{\frac{\alpha}{\beta}}^{k\tau_z s_z}, J_{\frac{\beta}{\alpha}}^{k\tau_z s_z}, J_{\alpha\beta}^{k\tau_z s_z}\right) = \int_{A_k} \frac{\partial F_\tau}{\partial z}\frac{\partial F_s}{\partial z}\left(1, H_\alpha^k, H_\beta^k, \frac{H_\alpha^k}{H_\beta^k}, \frac{H_\beta^k}{H_\alpha^k}, H_\alpha^k H_\beta^k\right)dz$$